Discretely Tunable Semiconductor Lasers Suitable for Photonic Integration

Diarmuid C. Byrne, Jan Peter Engelstaedter, Wei-Hua Guo, Qiao Yin Lu, Brian Corbett, Brendan Roycroft, James O'Callaghan, F. H. Peters, and John F. Donegan, *Senior Member, IEEE*

***Abstract*—A sequence of partially reflective slots etched into an active ridge waveguide of a 1.5 μm laser structure is found to provide sufficient reflection for lasing. Mirrors based on these reflectors have strong spectral dependence. Two such active mirrors together with an active central section are combined in a Vernier configuration to demonstrate a tunable laser exhibiting 11 discrete modes over a 30 nm tuning range with mode spacing around 400 GHz and side-mode suppression ratio larger than 30 dB. The individual modes can be continuously tuned by up to 1.1 nm by carrier injection and by over 2 nm using thermal effects. These mirrors are suitable as a platform for integration of other optical functions with the laser. This is demonstrated by monolithically integrating a semiconductor optical amplifier with the laser resulting in a maximum channel power of 14.2 dBm from the discrete modes.**

***Index Terms*—Photonic integration, semiconductor lasers, semiconductor optical amplifiers, tunable lasers.**

I. Introduction

WIDELY tunable semiconductor lasers will play an important part in next generation optical networks. Tunable lasers are essential in wavelength-agile networks and as a means to reduce costs as sparing lasers in wavelength-division multiplexing (WDM) systems. New approaches to data transmission such as coherent WDM (CoWDM [1]) require discrete tuning between particular wavelength channels on a grid. There is additionally an urgent need to integrate semiconductor lasers with other optical components such as amplifiers, modulators and detectors [2]–[5] in order to reduce chip cost, system size, and complexity. Tunable lasers are also needed in other important markets such as trace gas detection for environmental emission motoring [6].

Laser operation requires optical feedback, which is conventionally obtained in a semiconductor Fabry–Pérot laser by cleaving the ends of the laser waveguide along either (0 1 1) or (0 1 -1) crystallographic planes to form two semireflecting facets. However, due to the need for cleavage, it is difficult to integrate these lasers with other optical components on a single chip.

Manuscript received October 30, 2008; revised February 3, 2009. First published May 15, 2009; current version published June 5, 2009.

D. C. Byrne, W.-H. Guo, Q. Y. Lu, and J. F. Donegan are with the Semiconductor Photonics Group, School of Physics and Centre for Telecommunication Value Driven Research (CTVR), Trinity College, Dublin 2, Ireland (e-mail: byrnedc@tcd.ie).

J. P. Engelstaedter, B. Corbett, B. Roycroft, and J. O'Callaghan are with the Tyndall National Institute and Centre for Telecommunication Value Driven Research (CTVR), Cork, Ireland.

F. H. Peters is with the Physics Department, University College Cork, Cork, Ireland.

Color versions of one or more of the figures in this paper are available online at http://ieeexplore.ieee.org.

Digital Object Identifier 10.1109/JSTQE.2009.2016981

Distributed-Bragg-reflector (DBR) lasers and distributed feedback (DFB) lasers, which employ a series of small refractive index perturbations to provide feedback, do not rely on cleaved facets, and therefore, can be integrated with optical amplifiers and modulators [4], [5]. However, complex processing with multiple epitaxial growth stages is required for fabricating these lasers. Another method to obtain feedback is to etch a facet. However, this approach is limited by difficulties in the smoothness and verticality of the etched facet, particularly, for structures based on InP materials.

Previously, it was shown that by introducing a shallow slot into the active ridge waveguide of a laser, the longitudinal modes of the Fabry–Perot (FP) cavity were perturbed according to the position of the slot with respect to the cleaved facets [7]–[9]. By judicious placement of a sequence of low-loss slots with respect to the facets, preselected FP modes could be significantly enhanced leading to robust single-frequency lasing with wide temperature stability [10], [11] as well as tuning with fast switching characteristics [12]. More recently, we have characterized the properties of slots that are etched more deeply, namely, to the depth of, but not through, the core waveguide containing the quantum wells [13]. In that case, the reflection of each slot is of the order of $\sim$1% with transmission of $\sim$80% and the slot will strongly perturb the mode spectrum of the FP cavity by creating subcavities. The loss introduced by the presence of the slot is compensated by gain in the laser. An array of such slots can provide the necessary reflectivity for the laser operation independent of a cleaved facet where the gain between the slots compensates for the slot loss producing an active slotted mirror region. Such a mirror has been used in conjunction with a cleaved facet permitting the integration of a photodetector with the laser [14].

In this paper, we use reflective slots and the associated mirrors as the platform technology for the realization of a facetless laser that can be tuned using differential current injection into different longitudinal sections. Furthermore, the integration of the tunable laser with an optical amplifier is also demonstrated. The electrical isolation between the different sections is made possible by the etched slots. The slots are realized by conventional photolithography and dry etching during the definition of the waveguide. As the technology is based on a generic single epitaxial growth stage and upon standard laser processing steps, it is compatible with implementation in a foundry.

II. Tunable Laser Design

The semiconductor laser employing etched slots as the front and back mirrors is shown schematically in Fig. 1(a). The laser

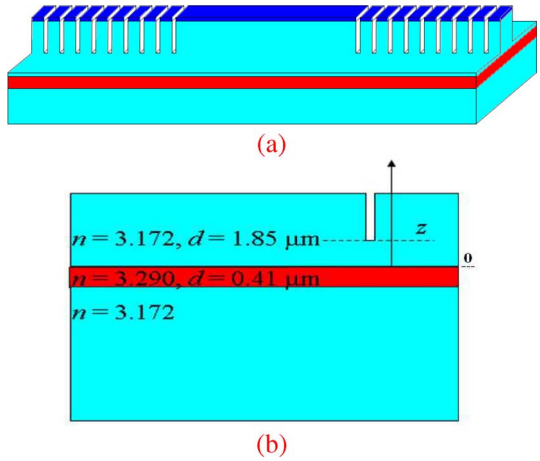

Fig. 1. (a) Schematic diagram of a laser with a series of slots as the front and back mirrors, both facets are angled to reduce facet reflections; (b) Cross section of single slot.

consists of a central gain section with separately contacted back and front mirror sections. The laser was fabricated with cleaved facets that were angled at 7° using a focused ion beam to minimize the reflections from the facet. The reflection from a single slot is relatively weak, so a series of slots distributed with a designed pattern is needed to provide sufficient feedback for lasing. However, because of the optical loss from the slot, the reflection from a group of slots will saturate quickly if the slot loss is not effectively compensated. In the design presented here, the mirror regions are also actively pumped, thus providing the necessary gain under current injection to compensate for the loss introduced by the slots.

In the following, the terms reflection and transmission refer to the field reflection and field transmission. The reflection from N equally spaced slots can be simply described by

$$r_t = r_s \frac{1 - t_s^{2N}\exp(gNl)\exp(-j2kn_{\text{eff}}Nl)}{1 - t_s^2\exp(gl)\exp(-j2kn_{\text{eff}}l)} \qquad (1)$$

where r_s and t_s are the reflection and transmission of a single slot, r_t is the total reflection from the slot group, g is the net modal gain of the active waveguide between slots, l is the slot spacing, $k = 2\pi/\lambda$ is the wave number in vacuum, and n_{eff} is the effective index of the active waveguide. Thus, equally spaced slots will produce a periodic reflection spectrum with the free spectral range (FSR) determined by the slot spacing $\Delta\lambda = \lambda^2/(2n_g l)$, where $n_g = n_{\text{eff}} - \lambda dn_{\text{eff}}/d\lambda$ is the group index of the active waveguide.

The maximum value and width of each reflection peak in the reflection spectrum is determined by the number of slots and the slot loss compensation level, which is determined by the factor $\gamma = t_s^2\exp(gl)$. Full slot loss compensation (i.e., all loss introduced by the slot is compensated by the gain in the regions between the slots) with $\gamma = 1$ results in the narrowest reflection peak. Fig. 2(a) shows the penetration depth of the field into the slot region normalized by the slot spacing, the full-width at half-maximum (FWHM) of the reflection peak normalized by the FSR, and the maximum value of the reflection peak normalized by the individual slot reflection versus the slot loss

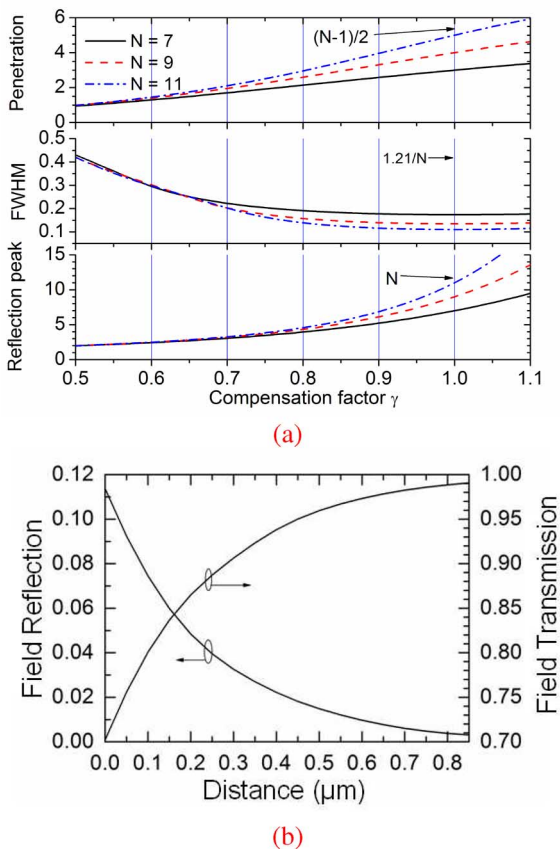

Fig. 2. (a) Penetration depth into the mirror section normalized to the slot period, FWHM of the reflection peak normalized to the FSR, and maximum values of the reflection peak normalized to the single-slot reflection versus the slot loss compensation factor for different number of equally spaced slots; (b) field reflection and transmission of the single slot versus the slot depth represented by the distance between the bottom of the slot and the top of the waveguide core.

compensation factor γ for different numbers of slots. As can be seen from the figure, if the slot loss is strongly undercompensated ($\gamma < 0.6$), an increasing number of slots results in little difference in the reflection because the field decays quickly into the slot region. In the full compensation situation, the field penetrates halfway into the slot region and the reflection peak has a minimum normalized FWHM of approximately $1.21/N$, as calculated from (1). In the overcompensated regime, the peak reflection increases exponentially with the compensation factor γ and the number of slots.

In Fig. 1, the slot is assumed to be etched to the same depth as the waveguiding ridge. In practice, the slot depth can be accurately and independently controlled by use of etch stop layers and be used to adjust the reflection and transmission of the individual slots. Fig. 2(b) shows how the calculated reflection and transmission from a single slot changes with the etch depth [15]. A longitudinal cross section of a single slot simplified is schematically shown in Fig. 1(b). The refractive index of the waveguide core layer is taken as 3.290, which is an average value over the core layers including the multiquantum well region and the upper and lower optical confinement layers. The index of the InP cladding regions is taken as 3.172. It is seen that a deeper

slot yields a larger reflection as well as a smaller transmission or greater loss. The reference distance is from the top of the waveguide core [as shown in Fig. 1(b)] and a negative value would describe an etching into the waveguide core region.

The reflectivity spectrum of the mirror can be designed with specific spectral properties to allow the realization of single-mode lasers, multimode lasers with specified mode spacing, or tunable lasers.

The designed laser consists of a central gain section that has a length of $500\ \mu$m, and a back and front mirror section having lengths of $972\ \mu$m and $873\ \mu$m, respectively. The gain section length of $500\ \mu$m was chosen to provide lots of gain as there are high losses associated with the etched slots; however, this length is not yet optimized. The total cavity length is $\sim 2345\ \mu$m. Each slot is nominally $0.88\ \mu$m in length in the longitudinal direction with nine slots in each mirror section. In order to employ the Vernier effect to improve the tuning range, the slots are spaced by $108\ \mu$m in the back mirror section and by $97\ \mu$m in the front mirror section. With a group index of 3.5, this yields an FSR in both reflectors of 3.36 and 3.02 nm, respectively. With this slot spacing, a discrete-mode hopping of 400 Ghz is achieved. The laser operates in a similar fashion to a surface grating Bragg reflector laser, as reported in [16]; however, due to the large distance between the slots ($\sim 100\ \mu$m), the mirror sections operates as a very high-order grating. The large distance between the slots is also beneficial in directly injecting carriers to these regions to produce active mirror sections.

Using the modeling results in Fig. 2(a), nine slots in both reflectors were chosen as a tradeoff between maximizing the reflectivity and minimizing the width of the reflection peaks while also ensuring that the length of the laser was kept to a minimum. A laser with 11 slots in each mirror would provide narrower bandwidth of reflection peak and a larger section reflection; however, the length of each mirror section would be over 1 mm in length. Assuming the slot transmission and reflection are 0.7 and 0.12, respectively (the slot is assumed to be etched to exactly above the waveguide core), the slot loss compensation factor can reach, for example, 0.8. This compensation level can be achieved with a net modal gain of around $47\ \text{cm}^{-1}$, which is the net mode gain required by a $250\ \mu$m long FP cavity laser with cleaved facets to reach threshold. Under this situation, the maximum value of the reflection peak is calculated to be 0.52, the FWHM of the reflection peak is 0.5 nm, and the penetration depth into the slot region is about $260\ \mu$m. So, the effective cavity length is about $1020\ \mu$m long and the longitudinal mode spacing covered by the reflection peak is about 0.32 nm, which is larger than half of the FWHM of the reflection peak. Based on this estimation, a good side-mode-suppression-ratio (SMSR) from the laser could be expected from the design. We also have some margin to reduce the number of slots in the mirror sections; especially, we can reduce the slot number in the front mirror section to help boost the output power of the laser.

III. Device Characterization

The tunable laser design described earlier was realized using the same fabrication steps as for a standard ridge waveguide laser. The laser epitaxial structure is a standard design employing an active region of 5 AlGaInAs quantum wells surrounded by InP n- and p-doped cladding regions. 2.5-μm-wide ridge waveguides were formed by inductively coupled plasma etching using Cl_2/N_2 gas. The slots are etched simultaneously with the ridge to a depth just into the waveguide core. The sidewalls are passivated with SiO_2 and an opening is made to the top of the ridge where a patterned Ti/Pt/Au electron-beam-evaporated ohmic contact is formed by lift-off lithography. The etched slot is sufficient to isolate the different longitudinal sections of the device allowing independent current injection. Following thinning of the substrate to $120\ \mu$m, an Au/Ge/Ni/Au contact is evaporated on to the n-type substrate. The devices are cleaved to the desired lengths and a single-layer antireflection coating applied to the facets.

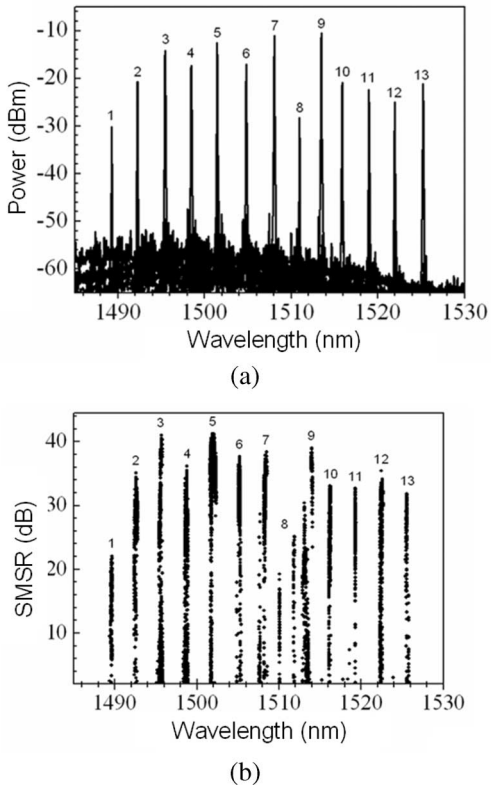

Fig. 3. (a) Measured fiber-coupled power spectra for all the discrete modes under different current settings; (b) measured SMSR versus wavelength for all the discrete modes under different current settings.

Three current sources were used to independently inject current into the gain and two mirror sections of the laser. The device was mounted on a heat sink and held at a constant temperature of $20\ ^\circ$C using a thermoelectric cooling unit. The current injected into the central gain section is fixed at 100 mA. The currents into the front and back mirror sections were scanned between 10 and 100 mA with a step of 1 mA. The wavelength and peak power of the laser emission spectrum and the SMSR were recorded using an optical spectrum analyzer with a resolution bandwidth of 0.1 nm.

Fig. 3(b) shows the fiber-coupled output power spectra under different current settings. Relatively large power variations

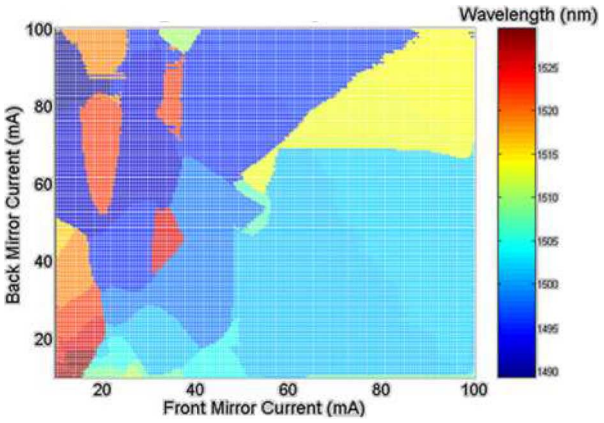

Fig. 4. Wavelength tuning map versus both mirror section injection currents.

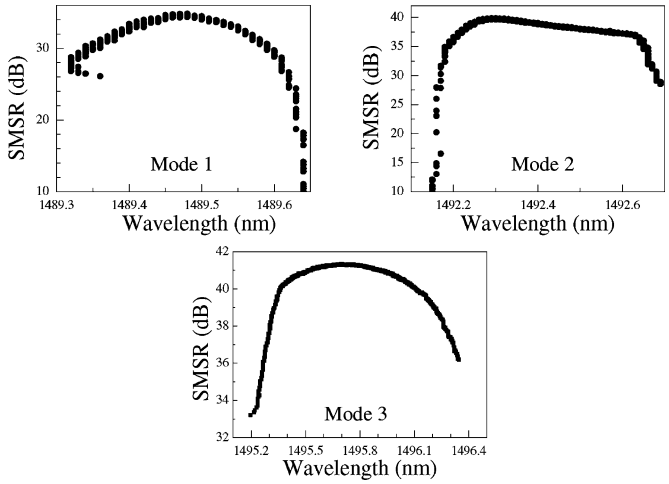

Fig. 5. Measured SMSR versus tuning wavelength due to a linear decrease in both mirror currents. Modes 1–3 refer to modes 1–3 from Fig. 1. (b).

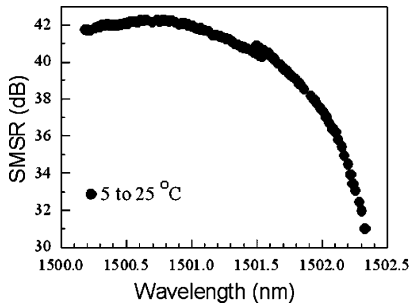

Fig. 6. SMSR versus wavelength for discrete-mode five with change in substrate temperature from 5 °C to 25 °C. The temperature is increased linearly from left to right.

can be seen mainly because the front mirror current has been changed significantly in the scan in order to fully explore the tuning characteristics of the laser. Fig. 3(b) shows a diagram of the wavelength peaks and their corresponding SMSRs. A discrete tuning behavior can be clearly seen over a tuning range of over 30 nm. With this experimental arrangement, a total of 13 discrete wavelengths can be accessed with a wavelength spacing around 3 nm, as expected for the present design. Eleven of the modes have an SMSR larger than 30 dB, except the first and eighth modes whose SMSR is around 20 dB. Fig. 4 shows a wavelength tuning map versus both mirror section injection currents. Discrete-mode hopping occurs at the boundaries of each different color section within this map. The threshold current is difficult to determine accurately as the device consists of three sections. However, when both mirror section injection currents are set for a particular mode, a threshold current of 56 mA in the gain section is observed. When all three sections are biased together, a threshold current of 146 mA is observed.

The continuous tuning characteristics of the modes due to change in injection current was investigated. The evolution of the SMSR versus wavelength of the first three discrete modes is shown in Fig. 5. These modes exhibit a continuous tuning of 0.27, 0.51, and 1.1 nm, respectively, which allow for accurate setting of the laser to precise optical frequencies. The continuous tuning of these modes by current injection suggests that full carrier clamping does not take place in the mirror sections of this laser. In comparison, an SGDBR laser has a continuous tuning range of <0.4 nm for all discrete modes, which is limited by the longitudinal-mode spacing, although its quasi-continuous tuning range is much greater [17], [18].

Fig. 6 shows the evolution of the wavelength and the associated SMSR due to thermal effects associated with a change of heat sink temperature from 5 °C to 25 °C; here, the temperature is varied linearly over this range increasing from left to right in Fig. 6 shown later. A continuous tuning of over 2 nm while maintaining an SMSR of over 30 dB is measured. The change in wavelength with temperature is in line with the change in the index of InP which is $1.9 \times 10^{-4}/\mathrm{K}$.

IV. Integration of an Optical Amplifier

As observed, there is a tradeoff between the wavelength tuning range and variations in the output power due to the requirements on the injection current in the output mirror section. To both increase and to balance the output power between the different wavelength channels, a semiconductor optical amplifier (SOA) is desired. This is provided by monolithically integrating an SOA with the tuneable laser source. The SOA consists of a 645-μm-long waveguide section on the output section of the tuneable laser. The SOA waveguide is curved to meet the output facet at an angle of 6°. This, together with an antireflection coating, is used to reduce backreflections into the laser section. The rear section of the laser is terminated by a 746-μm-long absorber section and an antireflection coated facet. This could also be used as an integrated photodetector. Fig. 7(a) shows a schematic of the integrated tuneable laser/SOA chip with four electrical sections. Fig. 7(b) shows the output characteristics of the device with seven wavelength channels spaced 400 GHz apart. The optical output power is significantly increased by the SOA with channel powers ranging from 10 to 14.2 dBm. All seven channels exhibit an SMSR greater than 30 dB with a maximum SMSR of approximately 40 dB.

Depending on the application of the wavelength tunable laser, only small variations of the output power of different

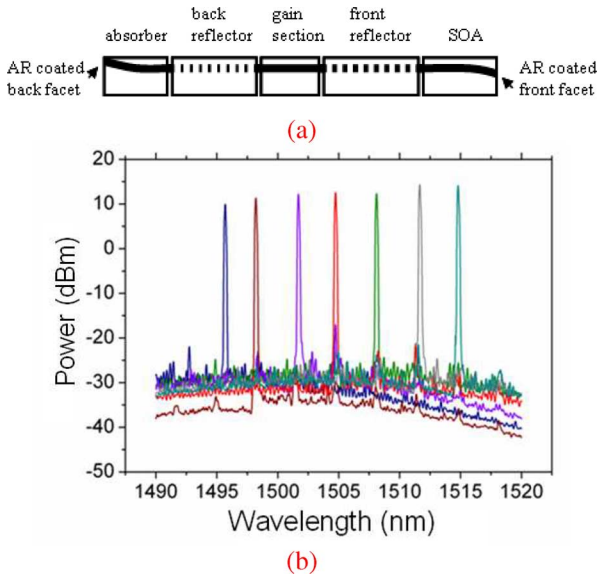

Fig. 7. (a) Schematic diagram of the integrated tunable laser with SOA; (b) seven selected wavelength channels accessible by the laser integrated with an SOA with maximum channel power of 14.2 dBm and a maximum SMSR of ~40 dB.

wavelength channels can be tolerated. With the integrated SOA, power equalization of six of the seven wavelength channels was demonstrated. The power flatness achieved was 1 dB. However, this value is not determined by the SOA dynamic range but by the degree of control over the laser wavelength tuning. In this device, thermal crosstalk becomes significant due to the close proximity of laser and SOA with high drive current into the SOA. Heat generated in the SOA heats the front mirror of the laser, changing the local refractive index and, in turn, the mirror reflectivity spectrum and laser output wavelength. This means that changing the laser output power not only requires a change in the amplifier drive current but also reprogramming of the laser tuning currents. This adds an additional dimension to the laser control problem. The wavelength is controlled through a lookup table that links wavelength and output power with the required tuning and amplifier currents and which has to be acquired experimentally. Power equalization can be improved by increasing the amount of points used in the lookup table.

V. Conclusion

We have demonstrated discretely tunable single-mode lasers realized by a single epitaxial growth stage by etching a sequence of slots into a ridge waveguide and using the Vernier tuning mechanism. We have achieved single-mode lasing with access to 11 modes, all with SMSR of over 30 dB, up to 1.1 nm continuous tuning by carrier density tuning and over 2 nm by thermal tuning. The demonstration of the monolithic integration of the tunable laser with an SOA indicates that this platform has strong potential for use as an integrated transmitter in high-volume optical communications.

References

[1] T. Healy, F. C. Garcia Gunning, A. D. Ellis, and J. D. Bull, "Multi-wavelength source using low drive-voltage amplitude modulators for optical communications," *Opt. Exp.*, vol. 15, pp. 2981–2986, 2007.

[2] L. A. Coldren, "Monolithic tunable diode lasers," *IEEE J. Sel. Topics Quantum Electron.*, vol. 6, no. 6, pp. 988–999, Nov./Dec. 2000.

[3] D. F. Welch, F. A. Kish, R. Nagarajan, C. H. Joyner, J. R. P. Schneider, V. G. Dominic, M. L. Mitchell, S. G. Grubb, T.-K. Chiang, D. D. Perkins, and A. C. Nilsson, "The realization of large-scale photonic integrated circuits and the associated impact on fiber-optic communication systems," *J. Lightw. Technol.*, vol. 24, no. 12, pp. 4674–4683, Dec. 2006.

[4] A. J. Ward, D. J. Robbins, G. Busico, E. Barton, L. Ponnampalam, J. P. Duck, N. D. Whitbread, P. J. Williams, D. C. J. Reid, A. C. Carter, and M. J. Wale, "Widely tunable DS-DBR laser with monolithically integrated SOA: Design and performance," *IEEE J. Sel. Topics Quantum Electron.*, vol. 11, no. 1, pp. 149–156, Jan./Feb. 2005.

[5] J. W. Raring and L. A. Coldren, "40-Gb/s widely tunable transceivers," *IEEE J. Sel. Topics Quantum Electron.*, vol. 13, no. 1, pp. 3–14, Jan./Feb. 2007.

[6] R. Phelan, M. Lynch, J. F. Donegan, and V. Weldon, "Simultaneous multi-species gas sensing by use of a sampled grating distributed Bragg reflector and modulated grating Y laser diode," *Appl. Opt.*, vol. 44, pp. 5824–5831, 2005.

[7] L. Coldren and T. Koch, "Analysis and design of coupled-cavity lasers—Part I: Threshold gain analysis and design guidelines," *IEEE J. Quantum Electron.*, vol. QE-20, no. 6, pp. 659–670, Jun. 1984.

[8] F. H. Peters and D. T. Cassidy, "Model of the spectral output of gain-guided and index-guided semiconductor diode lasers," *J. Opt. Soc. Amer. B*, vol. 8, pp. 99–105, 1991.

[9] B. Corbett and D. McDonald, "Single longitudinal mode ridge waveguide 1.3 μm Fabry–Perot laser by modal perturbation," *Electron. Lett.*, vol. 31, pp. 2181–2182, 1995.

[10] J. Patchell, D. Jones, B. Kelly, and J. O'Gorman, "Specifying the wavelength and temperature tuning range of a Fabry–Pérot laser containing refractive index perturbations," *Proc. SPIE*, vol. 5825, pp. 1–13, 2005.

[11] S. O'Brien and E. P. O'Reilly, "Theory of improved spectral purity in index patterned Fabry–Perot lasers," *Appl. Phys. Lett.*, vol. 86, pp. 201101-1–201101-3, 2005.

[12] R. Phelan, G. Wei-Hua, L. Qiaoyin, D. Byrne, B. Roycroft, P. Lambkin, B. Corbett, F. Smyth, L. P. Barry, B. Kelly, J. O'Gorman, and J. F. Donegan, "A novel two-section tunable discrete mode Fabry–Perot laser exhibiting nanosecond wavelength switching," *IEEE J. Quantum Electron.*, vol. 44, no. 4, pp. 331–337, Apr. 2008.

[13] B. Roycroft, P. Lambkin, S. Riesner, B. Corbett, and J. F. Donegan, "Transition from perturbed to coupled-cavity behavior with asymmetric spectral emission in ridge lasers emitting at 1.55 μm," *IEEE Photon. Technol. Lett.*, vol. 19, no. 2, pp. 58–60, Jan. 2007.

[14] J. P. Engelstaedter, B. Roycroft, and B. Corbett, "Laser and detector using integrated reflector for photonic integration," *Electron. Lett.*, vol. 44, pp. 1017–1019, 2008.

[15] Q. Y. Lu, W. H. Guo, R. Phelan, D. Byrne, J. F. Donegan, P. Lambkin, and B. Corbett, "Analysis of slot characteristics in slotted single-mode semiconductor lasers using the 2-D scattering matrix method," *IEEE Photon. Technol. Lett.*, vol. 18, no. 24, pp. 2605–2607, Dec. 2006.

[16] V. Jayaraman, Z. M. Chuang, and L. A. Coldren, "Theory, design, and performance of extended tuning range semiconductor lasers with sampled gratings," *IEEE J. Quantum Electron.*, vol. 29, no. 6, pp. 1824–1834, Jun. 1993.

[17] B. Mason, G. A. Fish, J. Barton, L. A. Coldren, and S. P. DenBaars, "Characteristics of sampled grating DBR lasers with integrated semiconductor optical amplifiers," in *Proc. Opt. Fiber Commun. Conf., 2000*, vol. 1, pp. 193–195.

[18] S. Oku, S. Kondo, Y. Noguchi, T. Hirono, M. Nakao, and T. Tamamura, "Surface-grating Bragg reflector lasers using deeply etched groove formed by reactive beam etching," in *Proc. 1998 Int. Conf. Indium Phosphide Relat. Mater.*, pp. 299–302.

Diarmuid C. Byrne was born in Donegal, Ireland, in 1983. He received the B.A. (mod) degree from the School of Physics, Trinity College, Dublin, Ireland, in 2005, where he is currently working toward the Ph.D. degree in physics. His current research interests include design, characterization, and applications of widely tunable semiconductor lasers.

Jan Peter Engelstaedter was born in Germany in 1980. He received the Dipl.-Ing. degree in electrical engineering and information technology from Aachen University of Technology (RWTH Aachen), Aachen, Germany, in 2006. He is currently working toward the Ph.D. degree in physics at the Tyndall National Institute and Center for Telecommunication Value Driven Research (CVTR), University College Cork, Cork, Ireland.

His current research interests include the modeling and design of tunable laser sources and the development of characterization techniques for such devices.

Wei-Hua Guo was born in Hubei Province, China, in 1976. He received the B.Sc. degree in physics from Nanjing University, Nanjing, China, in 1998, and the Ph.D. degree from the Institute of Semiconductors, Chinese Academy of Sciences, Beijing, China, in 2004.

His Ph.D. research was on finite-difference time-duration (FDTD) simulation and fabrication of optical microcavities and design of semiconductor optical amplifiers. Since September 2004, he has been a Postdoctoral Researcher in the Department of Physics, Trinity College, Dublin, Ireland. His current research interests include optimizing microcavity two-photon absorption photodetectors based on GaAs material system and designing tunable integrated sources for coherent wavelength-division multiplexing (WDM) systems.

Qiao Yin Lu was born in Jiangsu Province, China, in 1974. She received the B.Sc. and M.Sc. degrees in optics from the Changchun Institute of Optics and Fine Mechanics, Changchun, China, in 1998 and 2001, respectively, and the Ph.D. degree from the Institute of Semiconductors, Chinese Academy of Sciences, Beijing, China, in 2004, on the finite difference time duration (FDTD) simulation and fabrication of photonic microcavities.

She is currently a Postdoctoral Researcher with the School of Physics, Trinity College, Dublin, Ireland.

Brian Corbett received the B.A. (mod) degree in experimental physics and mathematics and the M.Sc. degree from Trinity College, Dublin, Ireland.

He is a Senior Research Scientist and Head of the III–V Materials and Devices Group, Tyndall National Institute and Center for Telecommunication Value Driven Research (CTR), Cork, Ireland. He has been engaged in developing extensive III–V micromachining expertise using dry and wet-etching techniques. This technology has been applied in both InP- and GaAs-based layer structures for devices such as low-cost single-frequency lasers as well as novel devices such as resonant cavity LEDs and photodetectors. His main research interest is in the use of geometry to define the optical properties of devices.

Brendan Roycroft was born in Ireland in 1970. He received the B.A.I. degree in microelectronic and electrical engineering, and the B.A. degree in mathematics and the Ph.D. degree in physics from Trinity College, Dublin, in 1993 and 1998, respectively.

He then designed, fabricated, and tested laterally coupled twin ridge lasers at the Optoelectronic Research Centre, Tampere, Finland, and in Spain at the Universidad Carlos III de Madrid. Since 2001, he has been with the Tyndall National Institute and Centre for Telecommunication Value Driven Research (CTVR), Cork, Ireland, as a Research Scientist. His current research interests include UV, green and red resonant cavity LEDs, red and near-IR vertical-cavity surface emitting lasers (VCSELs), and novel telecom lasers.

James O'Callaghan, photograph and biography not available at the time of publication.

F. H. Peters, photograph and biography not available at the time of publication.

John F. Donegan (M'04) received the B.Sc. and Ph.D. degrees in physics from the National University of Ireland, Galway, Ireland.

He held Postdoctoral positions in Lehigh University, Bethlehem, PA, and the Max Planck Institute, Stuttgart, Germany. He is currently a Professor of physics with Trinity College, Dublin, Ireland. His current research interests include photonic structures including broadly tunable lasers based on etched slots, microcavity two-photon absorption detectors, spherical microcavity structures, and photonic molecules. He also studies the interaction of quantum dots with human macrophage cells.

Prof. Donegan is a member of the American Physical Society, and a Fellow of the Institute of Physics and the Institute of Nanotechnology.